

# Powering Implants by Galvanic Coupling: A Validated Analytical Model Predicts Powers Above 1 mW in Injectable Implants

Marc Tudela-Pi<sup>✉</sup>, Laura Becerra-Fajardo<sup>✉</sup>, and Antoni Ivorra<sup>✉</sup>

## Abstract

While galvanic coupling for intrabody communications has been proposed lately by different research groups, its use for powering active implantable medical devices remains almost non-existent. Here it is presented a simple analytical model able to estimate the attainable power by galvanic coupling based on the delivery of high frequency (>1 MHz) electric fields applied as short bursts. The results obtained with the analytical model, which is in vitro validated in the present study, indicate that time-averaged powers above 1 mW can be readily obtained in very thin (diameter < 1 mm) and short (length < 20 mm) elongated implants when fields which comply with safety standards (SAR < 10 W/kg) are present in the tissues where the implants are located. Remarkably, the model indicates that, for a given SAR, the attainable power is independent of the tissue conductivity and of the duration and repetition frequency of the bursts. This study reveals that galvanic coupling is a safe option to power very thin active implants, avoiding bulky components such as coils and batteries.

## Keywords

Galvanic coupling • Active implant • Wireless power transfer

## 1 Introduction

Miniaturization of electronic medical implants has been hampered because of the use of batteries and inductive coupling for power. Both mechanisms require bulky and rigid parts which typically are much larger than the electronics they feed.

As we have recently shown in vivo [1], galvanic coupling can be an effective power transfer method which can lead to unprecedented implant miniaturization. Remarkably, although galvanic coupling for intrabody communications has been proposed lately by different research groups [2], its use for powering implants has remained almost non-existent. Reluctance to use galvanic coupling for power transfer may arise from not recognizing two facts. First, large magnitude high frequency (>1 MHz) currents can safely flow through the human body if applied as short bursts. Second, to obtain a sufficient voltage drop across its two intake (pick-up) electrodes, the implant can be shaped as a thin and flexible elongated body suitable for minimally invasive percutaneous deployment (Fig. 1a).

## 2 Methods

### 2.1 The Analytical Model and Its Rationale

Safety standards for human exposure to electromagnetic fields identify two general sources of risk regarding passage of radiofrequency (RF) currents through the body. On the one hand, the standards indicate risk of thermal damage due to the Joule effect, which roughly can be considered as frequency independent. On the other hand, the standards recognize risks caused by unsought electrical stimulation of excitatory tissues. In this case, safety thresholds increase with frequency. In particular, for frequencies above 1 MHz and short bursts, the IEEE standard [3] specifies limitations related to heating which are more restrictive than those

M. Tudela-Pi · L. Becerra-Fajardo · A. Ivorra  
Department of Information and Communication Technologies,  
Universitat Pompeu Fabra, 08018 Barcelona, Spain  
e-mail: marc.tudela@upf.edu

A. Ivorra (✉)  
Serra Hünter Fellow,  
Universitat Pompeu Fabra, 08018 Barcelona,  
Spain  
e-mail: antoni.ivorra@upf.edu

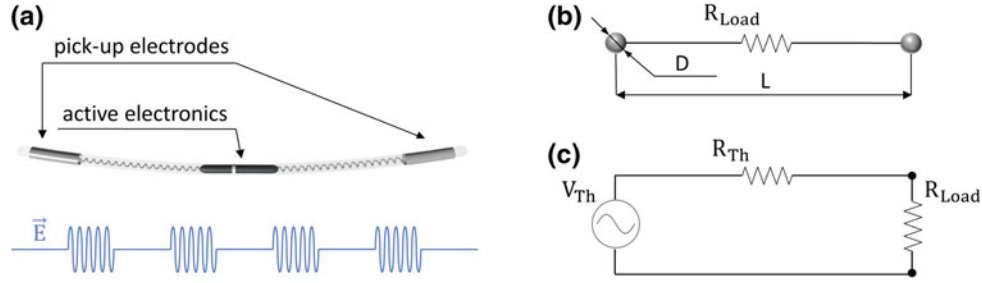


**Fig. 1** a We envision thin and flexible implants powered by innocuous high frequency current bursts through tissues. b Simplified model of the implant; D, electrode diameter; L, implant length. c Equivalent

Thévenin circuit for the conductive medium and the field, connected to the implant circuitry modeled as a resistive load

related to stimulation. Therefore, here only the thermal limitation is considered as we deem that frequencies between 1 and 10 MHz will be adequate for galvanic coupling. (Because of the skin effect, frequencies above 10 MHz may not be convenient as at that frequency the effect becomes significant [4] and the operation of implants at deep locations would be hindered.)

The limitations specified by the standards regarding heating are indicated as a limitation to the so-called Specific Absorption Rate (SAR), which can be calculated as:

$$\text{SAR} = \frac{\sigma(E_{\text{rms}})^2}{\rho} \quad (1)$$

where  $\sigma$  (S/m) is the electrical conductivity of the tissue,  $\rho$  ( $\text{kg/m}^3$ ) is the mass density of the tissue and  $E_{\text{rms}}$  is the root mean square value of the applied electric field (V/m). For occupational exposure or persons in controlled environments—as would be the case considered here—this limit is 10 W/kg.

If the field is applied as sinusoidal bursts (duration = B, repetition rate = F):

$$\text{SAR} = \frac{\sigma(E_{\text{peak}})^2}{2\rho} \text{FB} \quad (2)$$

where  $E_{\text{peak}}$  is the amplitude of the sinusoidal burst. Then, assuming a homogeneous medium and a uniform electric field, the maximum peak voltage across two points a and b at a separation distance L, is:

$$\begin{aligned} V_{\text{ab\_peak}} &= \overrightarrow{E_{\text{peak}}} \cdot \overrightarrow{r_{\text{ab}}} = E_{\text{peak}} L \cos(\theta) \\ &= \sqrt{\frac{2\rho\text{SAR}_{\text{max}}}{\sigma\text{FB}}} L \cos(\theta) \end{aligned} \quad (3)$$

where  $\overrightarrow{r_{\text{ab}}}$  is the vector defined by the points a and b and  $\theta$  is the angle between this vector and the field. If these two points correspond to the location of the two intake (pick-up) electrodes of the implant—here simply modeled as spheres

—then the rms open circuit voltage (i.e. the voltage across the electrodes in Fig. 1b if  $R_{\text{Load}} = \infty$ ) is:

$$V_{\text{OC\_rms}} = \frac{V_{\text{ab\_peak}}}{\sqrt{2}} \sqrt{\text{FB}} = \sqrt{\frac{\rho\text{SAR}_{\text{max}}}{\sigma}} L \cos(\theta) \quad (4)$$

And assuming that the implant is aligned with the electric field ( $\theta = 0$ ):

$$V_{\text{OC\_rms}} = \sqrt{\frac{\rho\text{SAR}_{\text{max}}}{\sigma}} L \quad (5)$$

If the implant circuitry is simply modeled as a load ( $R_{\text{Load}}$ ), then it is straightforward to compute the maximum power that it will dissipate if the Thévenin resistance ( $R_{\text{Th}}$ ) of the Thévenin equivalent circuit (Fig. 1c) is known:

$$P_{\text{Load\_max}} = P_{\text{Load}}(\text{if } R_{\text{Load}} = R_{\text{Th}}) = \frac{V_{\text{OC\_rms}}^2}{4R_{\text{Th}}} \quad (6)$$

For an infinite medium (i.e. the electrodes that deliver the field are far away),  $R_{\text{Th}}$  is the resistance across the two implant electrodes. If the implant electrodes are modeled as spheres with a separation distance much larger than the diameter ( $L \gg D$ ), then [5]:

$$R_{\text{Th}} = \frac{1}{\sigma\pi D} \quad (7)$$

Therefore, the maximum average power for a given SAR limit ( $\text{SAR}_{\text{max}}$ ) that can be drawn by the implant is:

$$P_{\text{Load\_max}} = \frac{V_{\text{OC\_rms}}^2}{4R_{\text{Th}}} = \frac{\pi}{4} \text{SAR}_{\text{max}} \rho D L^2 \quad (8)$$

## 2.2 Experimental Setup

An in vitro experimental setup that replicates the assumptions made to generate the previous model was developed to validate the analytical expression in (8), (Fig. 2).

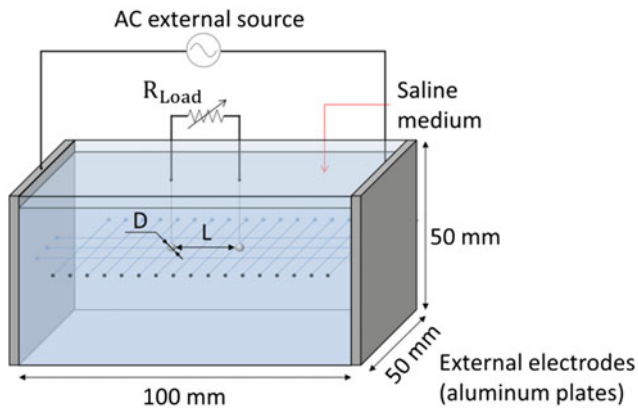


**Fig. 2** Schematic representation of the in vitro setup developed to validate the analytical model (see text for details). For geometrical reference, a 0.5 cm  $\times$  0.5 cm grid made of cotton thread was sewed across the plates, 2.5 cm from the bottom of the structure

The field was delivered by two 5 cm  $\times$  5 cm parallel aluminum plates held at a distance of 10 cm using two polycarbonate plates. 1 MHz voltage bursts across these two electrodes were generated by the combination of a function generator (4060 Series by BK Precision) and a high voltage amplifier (WMA 300 by Falco systems).

The above electrode structure was placed inside a 19 cm  $\times$  14 cm  $\times$  6.3 cm glass container, which was filled with a saline solution. Three different concentrations were tried: 0.3, 0.6 and 0.9% NaCl. The conductivity of these solutions at 20 °C, as measured with a conductivity tester (HI 98312 by Hanna), was 0.58 S/m, 1.1 S/m and 1.56 S/m respectively.

The magnitude of the applied voltage was adjusted for a SAR of 10 W/kg according to expression 2.

The pick-up electrodes of the implants were modeled by stainless steel spherical electrodes (SAE 316) with four different diameters: 0.5, 1, 1.5, and 2 mm. Each electrode was laser welded to a 10 cm piece of 32 AWG enameled copper wire.

In each trial, a pair of electrodes with the same diameter was connected to a 1 k $\Omega$  high-precision potentiometer ( $R_{Load}$  in Fig. 2). The potentiometer was adjusted in advance to the computed  $R_{Th}$  value in order to draw the maximum possible power.

Instant power dissipated at the potentiometer was computed as the square of the recorded voltage across it, using an oscilloscope (TPS2014 by Tektronix Inc.), divided by the

value of  $R_{Load}$ . Power was then time averaged for the burst repetition period (i.e. average power) and for the duration of the burst (i.e. peak power).

### 3 Results and Discussion

Figure 3 shows a set of numerical results from the analytical model (expression 8) together with the corresponding experimental results. As it can be observed, the experimental results fit the analytical model and powers above 1 mW are obtained for all the diameters when the inter electrode distance ( $L$ ) is larger than 2 cm.

Expression 8 indicates that the maximum time-averaged power than can be drawn by the implant is independent of the duration ( $B$ ) and the repetition frequency ( $F$ ) of the bursts. However, the same does not apply for the maximum power that can be drawn during the burst (peak power). This is illustrated in Fig. 4d where it is modeled the delivery of three different burst patterns (Fig. 4a–c) with a rms value of 141 V/m ( $D = 1$  mm, SAR = 10 W/kg, and  $\rho = 1000$  kg/m<sup>3</sup>). Since the power increases with the square of the applied voltage, peak powers of hundreds of mW can be obtained when short burst ( $B < 1$  ms) are applied.

Remarkably, the analytical model (expression 8) indicates that, for a given SAR, the attainable power is independent of the tissue conductivity. This is validated in Fig. 4e where experimental results are displayed for three different conductivities ( $\sigma_{0.9\%} = 1.56$  S/m,  $\sigma_{0.6\%} = 1.1$  S/m, and  $\sigma_{0.3\%} = 0.58$  S/m).

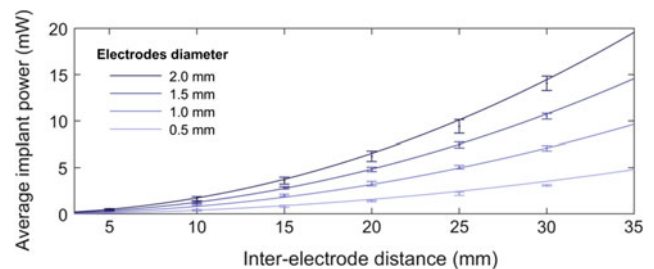


**Fig. 3** Time-averaged power dissipated at  $R_{Load}$  for different electrodes diameters ( $D$ ) and inter-electrode distances ( $L$ ). Solid lines correspond to the analytical model (expression 8). Bars correspond to the 95% confidence interval of 10 experimental measurements. Experimental parameters:  $\sigma = 0.58$  S/m (0.3% NaCl),  $\rho = 1000$  kg/m<sup>3</sup> (water),  $V_{rms} = 13.1$  V,  $R_{Load} = 549$   $\Omega$

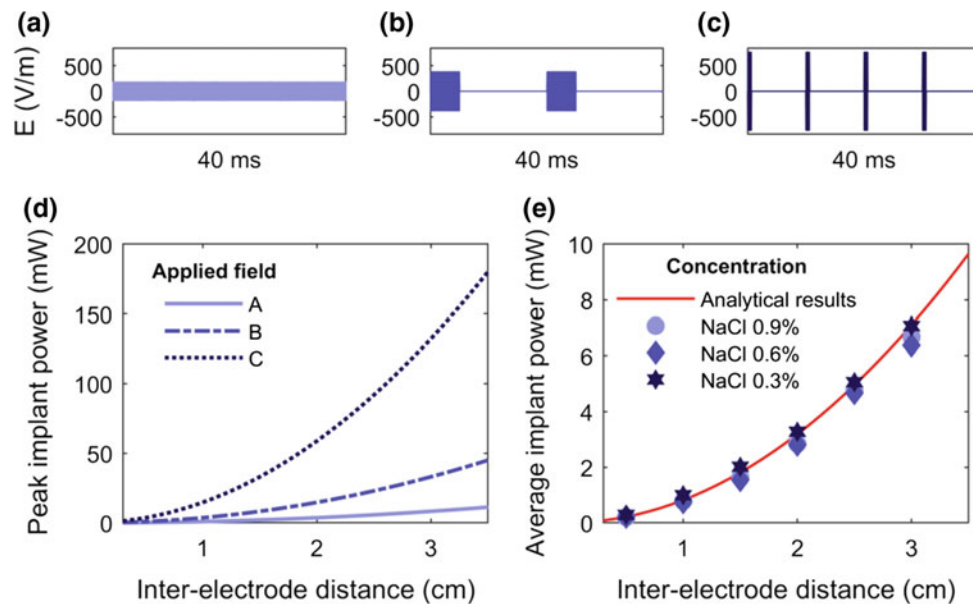


**Fig. 4** Dependences on the burst pattern and the media conductivity. **a** Continuous 1 MHz 141  $V_{\text{rms}}/m$  sinusoidal field,  $E_{\text{Peak}} = 200$  V/m. **b** Bursts of 1 MHz 141  $V_{\text{rms}}/m$  sinusoidal field  $B = 5$  ms,  $F = 50$  Hz,  $E_{\text{Peak}} = 400$  V/m. **c** Bursts of 1 MHz 141  $V_{\text{rms}}/m$  sinusoidal field

$B = 625$   $\mu\text{s}$ ,  $F = 100$  Hz,  $E_{\text{Peak}} = 800$  V/m. **d** Predicted peak power attainable in an implant ( $D = 1$  mm) for the burst patterns of subfigures A, B and C. **e** Modeled and experimentally obtained time-averaged powers for three conductivities ( $D = 1$  mm,  $\text{SAR} = 10$  W/kg)

## 4 Conclusions

The results of this study indicate that it should be possible to safely supply powers well above 1 mW to thin elongated ( $D \leq 1$  mm,  $L \geq 20$  mm) implants using galvanic coupling. For that, the energizing electric field—generated by an externally delivered current or voltage—can consist in a high frequency ( $>1$  MHz) sinusoidal wave applied in short bursts resulting in a SAR value below 10 W/kg.

The predicted time-averaged powers ( $>1$  mW) are one to three orders of magnitude above the requirements of some implantable technologies for sensing and stimulation [6], including conventional pacemakers (10 to 50  $\mu\text{W}$ ).

Remarkably, the developed analytical model predicts that, for a given SAR, the attainable power is independent on the tissue conductivity and on the duration and repetition frequency of the bursts. These predictions are experimentally confirmed by the in vitro model that replicates the assumptions made to generate the analytical model.

Peak powers in the order of tens or hundreds of mW are attainable when bursts are very short in comparison to their repetition period. This suggests that galvanic coupling may be particularly useful in applications requiring large amounts of power in short intervals, such as is the case of neuromuscular stimulation [1].

**Acknowledgements** This project has received funding from the European Research Council (ERC) under the European Union’s Horizon 2020 research and innovation programme (grant agreement No 724244).

**Conflict of Interest** The authors declare no conflict of interest.

## References

1. Becerra-Fajardo, L., Schmidbauer, M., Ivorra, A.: Demonstration of 2 mm thick microcontrolled injectable stimulators based on rectification of high frequency current burst. *IEEE Trans Neural Sys. Rehabil. Eng.* 25(8), 1342–52 (2017).
2. Seyedi, M., Kibret, B., Lai, D.T.H., Faulkner, M.: A survey on intrabody communications for body area network applications. *IEEE Trans. Biomed. Eng.* 60(8), 2067–79 (2013).
3. IEEE Standard for Safety Levels With Respect to Human Exposure to Radio Frequency Electromagnetic Fields, 3 kHz to 300 GHz. 1–238 (2006).
4. Vander Vorst, A., Rosen, A., Kotsuka, Y.: *RF/Microwave Interaction with Biological Tissues*. New Jersey: John Wiley & Sons, Inc. (2006).
5. Grimnes, S., Martinsen, Ø.G., *Geometrical Analysis*, in: *Bioimpedance & Bioelectricity basics*. 2nd edn. Elsevier, Oxford (2008).
6. Ho, J.S. et al., Supplementary material in: Wireless power transfer to deep-tissue microimplants. *Proc. Natl. Acad. Sci.* 111, 7974–7979 (2014).